

Influence of the upper Layers of the Sun on the p -mode Frequencies

J. Christensen-Dalsgaard ^a, F. Pérez Hernández ^b

^aInstitute for Theoretical Physics, University of California,
Santa Barbara; and Astronomisk Institut, Aarhus Universitet,
DK 8000 Aarhus C, Denmark¹

^bInstituto de Astrofísica de Canarias, E-38200, La Laguna, Tenerife, Spain

Abstract: We consider the effect of uncertainties in solar models on the p -mode frequencies of moderate degree ($40 \leq l \leq 100$). This is done by means of an asymptotic relation that provides a simple way of estimating differences in p -mode frequencies of two solar models. Also, we have investigated the possibility for separating different contributions to the difference between the models, on the basis of the frequencies of the modes. Analysis of observed frequencies suggests that the solar envelope helium abundance Y_e is close to 0.25; however, this result may be sensitive to other uncertainties in the solar models.

1 Introduction

Asymptotic relations have been used with success to invert the observed p -mode frequencies to obtain estimates of the local sound speed throughout most of the Sun. However, these relations are not strictly valid near the surface, where the scale heights of pressure and density are small compared with the wavelength of the modes. Therefore, to study these layers, which have considerable influence on the p -mode frequencies, different techniques are required. Here we consider the frequency-dependence of the phase shift resulting from the reflection of the modes near the surface. As shown by, for example, Christensen-Dalsgaard & Pérez Hernández (1988) and Brodsky & Vorontsov (1988) this is sensitive to the properties of the outer layers of the Sun. We demonstrate this by analyzing differences between models differing in various aspects of the physics of these layers. On the basis of the results, a similar analysis of observed frequencies is interpreted in terms of errors in the solar models.

¹ Permanent address

2 Background

Asymptotically, frequency differences between p -modes of two models calibrated to the same radius satisfy to first order the relation (Christensen-Dalsgaard, Gough & Pérez Hernández 1988)

$$S_{nl} \frac{\delta\omega_{nl}}{\omega_{nl}} \simeq \int_{r_t}^{R_{ph}} \left(1 - \frac{L^2 c^2}{r^2 \omega^2}\right)^{-1/2} \frac{\delta c}{c} \frac{dr}{c} + \frac{\pi}{\omega} \delta\alpha(\omega), \quad (1)$$

where

$$S_{nl} = \left[\int_{r_t}^{R_{ph}} \left(1 - \frac{L^2 c^2}{r^2 \omega^2}\right)^{-1/2} \frac{dr}{c} \right] - \pi \frac{d\alpha}{d\omega}. \quad (2)$$

Here ω is the frequency, l and n are degree and radial order of the mode, $L = l + 1/2$, c is the sound speed, R_{ph} the photospheric radius, and r_t the inner turning point determined by $r_t/c(r_t) = L/\omega$. – For any quantity f , $\delta f = f^{(2)} - f^{(1)}$ (at fixed r , if f depends on r) where (1) and (2) refer to the two models.

The first term on the right hand side of (1) is a function $H_1(\omega/L)$ of ω/L . Also, as indicated, the effective phase $\alpha(\omega)$, which takes into account the influence of the upper layers, is expected to be a function of ω but not of l . The frequency-dependent term in (1) may be written as

$$H_2(\omega) \equiv \frac{\pi}{\omega} \delta\alpha(\omega) \simeq \int_{r_0}^R \left\{ K_{\omega}^{(c)}(r) \frac{\delta c}{c}(r) + K_{\omega}^{(\omega_a)}(r) \frac{\delta\omega_a}{\omega_a}(r) \right\} dr \quad (3)$$

(Christensen-Dalsgaard & Pérez Hernández 1988, 1990). Here $\omega_a = c/(2H_p)$, where H_p is the pressure scale height, r_0 is a point in the adiabatically stratified part of the convection zone and R is the point where the surface boundary conditions on the oscillations are applied. $K_{\omega}^{(c)}(r)$ and $K_{\omega}^{(\omega_a)}(r)$ are kernels that may be computed from the reference model.

In the adiabatically stratified part of the convection zone, and inside the dominant ionization zones of hydrogen and helium, $\delta c(r) \simeq 0$ for a wide range of perturbations to the structure of the model (*e.g.* Christensen-Dalsgaard 1988). Therefore, for modes with turning points within the convection zone, but well beneath the the second He-ionization region, one has that

$$S_{nl} \frac{\delta\omega_{nl}}{\omega_{nl}} \simeq \int_{r_0}^{R_{ph}} \frac{\delta c}{c} \frac{dr}{c} + H_2(\omega). \quad (4)$$

We restrict our work to modes that satisfy (4). Since the first term on the right hand side of (4) is independent of n and l , we expect $S_{nl}\delta\omega_{nl}/\omega_{nl}$ to be predominantly a function of frequency for these modes.

When comparing two models we consider the quantity $\langle S\delta\omega/\omega \rangle(\omega)$ obtained from the right hand side of (4), using (3) to determine H_2 . In comparisons with the observations we calculate eigenfrequencies that satisfy (4) and take averages $\langle S\delta\omega_{nl}/\omega_{nl} \rangle(\omega)$ over all the modes within frequency bins of width $100\mu\text{Hz}$. For pairs of models these two procedures give essentially the same results.

To calculate the quantities entering into (4) we need to know only the structure of the upper layers of the models; hence we can use envelope models rather than full evolution models. These models are faster to compute; furthermore, it is possible to introduce arbitrary values of the hydrogen abundance X_s and the mixing length parameter α_c . Except where otherwise noted, we use as reference model an envelope model with heavy element abundance $Z = 0.02$, the opacities of Cox, Guzik & Kidman (1989), the Eggleton, Faulkner & Flannery (1973; in the following EFF) equation of state and the values $X_s = 0.6967$ and $\alpha_c = 2.5442$ which correspond to those of an evolutionary model with the same physics.

3 Differences between models

Figures 1 – 4 give results for various modifications to the physics of the models. The error bars correspond to an estimate based on the observed frequencies, as indicated in Fig. 5.

Analysis of H_2 , as given by (3), shows that the contribution from the uppermost layers ($0.995R_\odot$ to $1R_\odot$) to the function $\langle S\delta\omega/\omega \rangle(\omega)$ depends smoothly on frequency, whereas the layers around the second He-ionization zone ($0.98R_\odot$ to $0.99R_\odot$) make a contribution with an oscillatory behaviour as a function of ω (Christensen-Dalsgaard & Pérez Hernández 1990). Hence, when two models differ only in the uppermost layers, the scaled frequency differences are smooth functions of ω ; furthermore it may be shown that their values at low ω are small.

3.1 Change in the hydrogen abundance

Figure 1 shows $\langle S\delta\omega/\omega \rangle(\omega)$ for a model where the hydrogen abundance has been increased by $\delta X_s/X_s = 0.04$, relative to the reference model. The oscillatory behaviour at low ω , associated with the second helium ionization zone and arising directly from the change in the composition, is evident. Over the range in X_s among normal solar models $\langle S\delta\omega/\omega \rangle(\omega)$ is very nearly proportional to δX_s ; therefore, for other values of δX_s the frequency differences can be obtained from those shown in Fig. 1 by means of a suitable scaling. It follows that for $|\delta X_s/X_s| \leq 0.01$ the frequency differences would be smaller than their errors. This provides an estimate of the precision with which X_s can be determined from an analysis of this nature, based on modes that satisfy (4).

3.2 Change in the surface opacity

Here the opacity in the atmosphere and upper part of the convection zone was increased by a factor 10^A , with $A = 0.2$. The resulting $\langle S\delta\omega/\omega \rangle(\omega)$, shown in Fig. 2, is a smooth function of frequency which is very small at low frequency. This is in accordance with the fact that the opacity plays a significant role only in the uppermost parts of the convection zone, where the radiative and convective

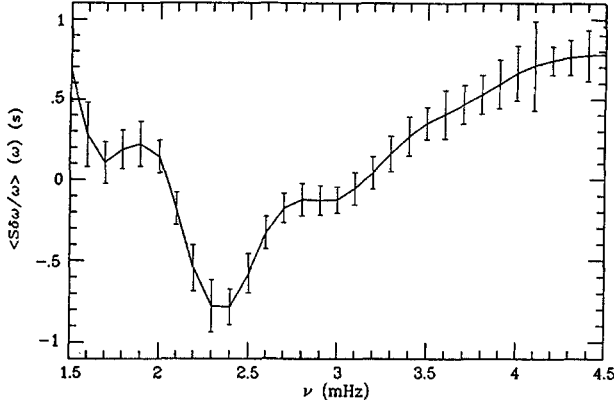


Fig. 1. Scaled frequency differences $\langle S\delta\omega/\omega \rangle(\omega)$, against the cyclic frequency $\nu = \omega/2\pi$, for two models that differ in the surface hydrogen abundance X_s by $\delta X_s/X_s = 0.04$. The models were calibrated to have the same depth of the convection zone.

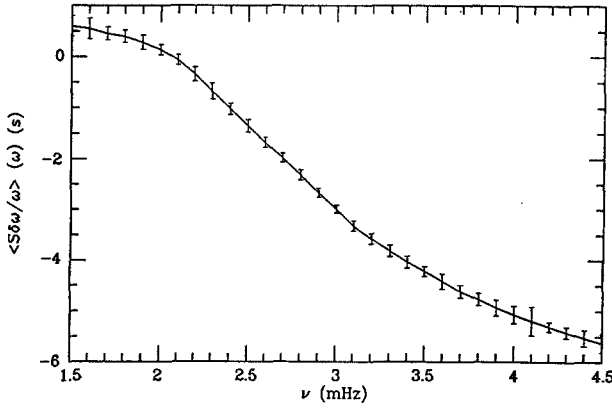


Fig. 2. The same as Fig. 1 but for a model where the opacity in the upper layers has been increased by a factor $10^{0.2}$; the models have the same depth of the convection zone.

transport are comparable, and in the atmosphere. $-\langle S\delta\omega/\omega \rangle(\omega)$ is proportional to A up to, at least, $A = 0.6$.

3.3 Change in the treatment of the superadiabatic gradient

We have considered a model with an artificial treatment of the superadiabatic gradient near the top of the convection zone (Christensen-Dalsgaard 1986), fixing the depth of the convection zone. The main difference, relative to the reference model, is that the superadiabatic region is substantially broader and less pronounced. The resulting $\langle S\delta\omega/\omega \rangle(\omega)$ is shown in Fig. 3.

To investigate whether the effects of this change can be separated from other changes, we have carried out a least squares fit to $\langle S\delta\omega/\omega \rangle(\omega)$ on the form

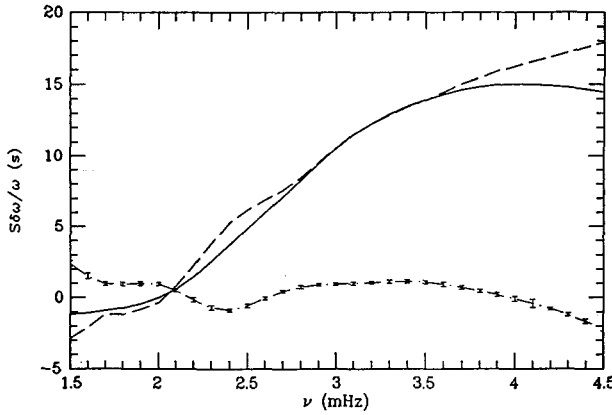


Fig. 3. The continuous line shows the $\langle S\delta\omega/\omega \rangle(\omega)$ resulting from modifying the superadiabatic gradient in the upper part of the convection zone. The dashed line shows an attempted fit to this by a combination of appropriately scaled $\langle S\delta\omega/\omega \rangle(\omega)$ for changes in opacity and hydrogen abundance, and the dot-dashed line shows the residual.

$$\left\langle S\frac{\delta\omega}{\omega} \right\rangle \simeq \left(\left\langle S\frac{\delta\omega}{\omega} \right\rangle \right)^{(fit)} = C_1 \left(\left\langle S\frac{\delta\omega}{\omega} \right\rangle \right)^{(X)} + C_2 \left(\left\langle S\frac{\delta\omega}{\omega} \right\rangle \right)^{(op)} \quad (5)$$

where $(\langle S\delta\omega/\omega \rangle)^{(X)}$ and $(\langle S\delta\omega/\omega \rangle)^{(op)}$ are the $\langle S\delta\omega/\omega \rangle$ corresponding to changes in X , and the opacity, as shown in Fig. 1 and 2. The dashed line shows the function $(\langle S\delta\omega/\omega \rangle)^{(fit)}$, and the dot-dashed line is the residual in the fit, the error bars corresponding to those for the observed frequencies. Clearly the error in the fit is larger than the observational errors. This offers some hope that data of this form may allow a separation of errors in the atmospheric opacity from errors in the superadiabatic gradient.

3.4 Changes in the equation of state

To test the effects of the equation of state, we have compared our reference model, which uses the EFF equation of state, with a model using the so-called MHD equation of state (for Mihalas, Hummer & Däppen; see Christensen-Dalsgaard, Däppen & Lebreton 1988 for a short description and further references). The change from EFF to MHD was shown by Christensen-Dalsgaard *et al.* to result in a significant improvement of the agreement between observed and computed frequencies. The resulting $\langle S\delta\omega/\omega \rangle(\omega)$ is shown in Fig. 4. There is evidently a substantial oscillatory component associated with the second helium-ionization zone.

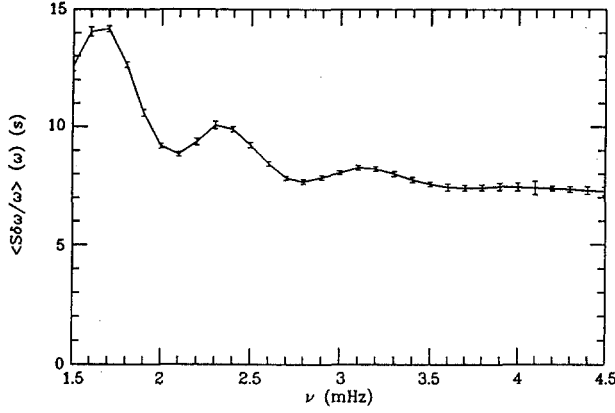


Fig. 4. The same as Fig. 1 but for two models that differ in the equation of state. The test model use the MHD equation of state (see text).

4 Comparison with observations

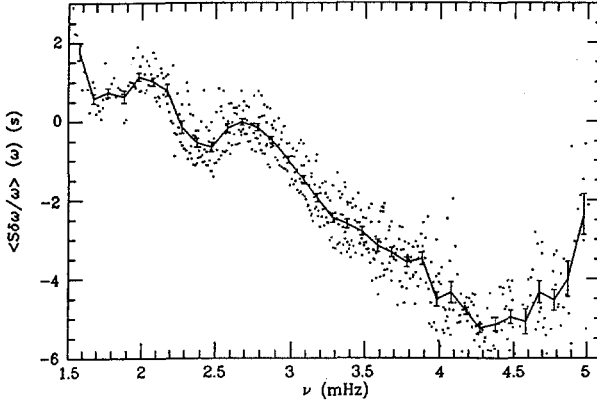


Fig. 5. Scaled frequency differences $S_{nl}\delta\omega_{nl}/\omega_{nl}$ (dots) between observed and computed frequencies. The continuous line shows the corresponding average frequency differences $\langle S\delta\omega_{nl}/\omega_{nl} \rangle(\omega)$. The errors are calculated as the uncertainties in the mean values.

We have compared the observed frequencies from Duvall *et al.* (1988) with frequencies for an envelope model with the MHD equation of state, but otherwise computed as the reference model of the preceding section; the value $\alpha_c = 2.555$ was chosen to obtain the same depth of the convection zone, $d_b = 0.267R_\odot$. Only modes with ν/L in the interval 30 to 60 μHz were included. Figure 5 shows the resulting scaled frequency differences.

The average $\langle S\delta\omega_{nl}/\omega_{nl} \rangle(\omega)$ contains a large component which is a smooth function of frequency; this indicates that a major source of errors is localized immediately beneath the photosphere. There is also a significant oscillatory behaviour at low ω which suggests errors in the layers beneath, say, $0.995R_\odot$.

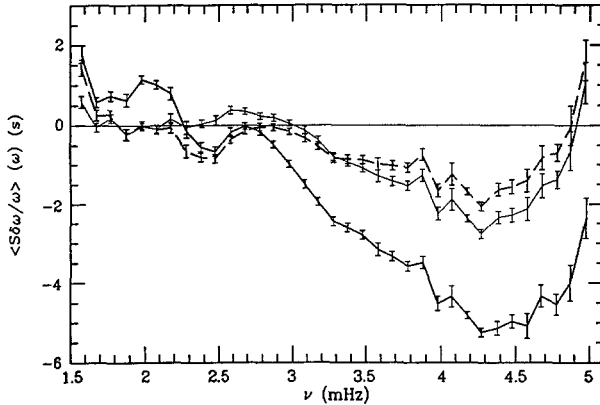


Fig. 6. Scaled differences $\langle S\delta\omega_{nl}/\omega_{nl} \rangle(\omega)$ between observed frequencies and those for three solar models. The heavy continuous line is the same as in Fig. 5. The heavy dashed line corresponds to differences for a solar model calibrated to the actual depth of the convection zone. The thin continuous line shows the frequency differences for a model where in addition $X_s = 0.727$.

To investigate this in more detail we have compared the observations with two additional models. In the first model (shown with a heavy dashed curve in Fig. 6) α_c was adjusted to fit the actual depth of the solar convection zone, $d_b = 0.287R_\odot$, as determined from sound-speed inversion (Christensen-Dalsgaard, Gough & Thompson 1991). This reduces the frequency differences, especially at high frequencies. At low frequency some oscillatory behaviour remains, which could be caused both by errors in the equation of state and in X_s . On the assumption that the latter dominate, we have fitted the results for $\nu \leq 3\text{mHz}$ to those obtained for modifications in X_s (cf. Fig. 1), yielding $X_s = 0.723 \pm 0.004$. The thin curve in Fig. 6 shows the differences for a model computed with $X_s = 0.727$. This removes the oscillatory behaviour at low frequencies. Hence, if the uncertainty in the equation of state is negligible, these data suggest that $X_s \approx 0.73$.

The remaining slowly varying discrepancy at high frequency has a significantly different shape from the differences resulting from changes in the opacity, or from the specific change in the superadiabatic gradient which we have considered here (cf. Fig. 2 and 3). Hence there are other sources of errors in the uppermost layers.

5 Discussion

It appears that changes in the opacity in the solar atmosphere and the layers just beneath the photosphere, in the description of the superadiabatic gradient in the upper part of the convection zone, in the composition, and in the assumed equation of state, have different signatures in the resulting frequency differences. The first two types of changes result in a frequency change that varies slowly with frequency and is small at low frequencies. The last two types of changes in addition give rise to an oscillatory component of the frequency change which is related to the helium

ionization zone. For none of the four cases considered the effect of a particular change can be approximated to within the accuracy of current observations by a linear combination of the remaining three. Thus it may be possible to separate these effects in the observed frequencies.

From analysis of observed frequencies we have found that $X_s \approx 0.73$, and hence the helium abundance is $Y_s \approx 0.25$. This is similar to the value found by Vorontsov, Baturin & Pamyatnykh (1990) from an independent analysis, closely related to ours, of the asymptotic phase α . Further investigation is required to evaluate the sensitivity of the result to other uncertainties in the solar models.

Our calculations neglect effects of "turbulent pressure" in the convection zone and of departures from adiabaticity. Such effects are probably concentrated very near the surface, and hence should give rise to a contribution to frequency difference which varies smoothly with ω . Therefore it is hardly surprising that the comparison in Fig. 6 between observed and computed frequencies shows differences that cannot be eliminated by changes in opacity, or modifications to the superadiabatic gradient of the form considered here.

This research was supported in part by the National Science Foundation under Grant No. PHY89-04035, supplemented by funds from the National Aeronautics and Space Administration, and by the Danish Research Council and the Danish Space Board.

References

- Brotsky, M. A. & Vorontsov, S. V., 1988. *Seismology of the Sun & Sun-like Stars*, p. 487, eds Domingo, V. & Rolfe, E. J., ESA SP-286.
- Christensen-Dalsgaard, J., 1986. In *Seismology of the Sun and the Distant Stars*, Dordrecht, D. Reidel Publ. Co., p. 23.
- Christensen-Dalsgaard, J., 1988. In *Seismology of the Sun and Sun-like Stars*, ESA SP-286, p. 431.
- Christensen-Dalsgaard, J. & Pérez Hernández F., 1988. In *Seismology of the Sun and Sun-like Stars*, ESA SP-286, p. 499.
- Christensen-Dalsgaard, J. & Pérez Hernández, F., 1990. In preparation.
- Christensen-Dalsgaard, J., Däppen, W. & Lebreton, Y., 1988. *Nature*, **336**, 634.
- Christensen-Dalsgaard, J., Gough D.O. & Pérez Hernández, F., 1988. *Mon. Not. R. astr. Soc.*, **235**, 875.
- Christensen-Dalsgaard, J., Gough D.O. & Thompson, M.J., 1991. *Astrophys. J.*, in the press.
- Cox, A.N., Guzik, J.A. & Kidman P.R., 1989. *Astrophys. J.*, **342**, 1187.
- Duvall T.L., Harvey, J.W., Libbrecht, K.G., Popp, B.D. & Pomerantz, M.A., 1988. *Astrophys. J.*, **324**, 1158.
- Eggleton, P.P., Faulkner, J. & Flannery, B.R., 1973. *Astr. Astrophys.*, **23**, 325.
- Vorontsov, S. V., Baturin, V. A. & Pamyatnykh, A. A., 1990. *Nature*, in the press.